

See discussions, stats, and author profiles for this publication at: <https://www.researchgate.net/publication/351125533>

A new framework for the identification of flash drought: multivariable and probabilistic statistic perspectives

Article in *International Journal of Climatology* · April 2021

DOI: 10.1002/joc.7157

CITATIONS

8

READS

368

6 authors, including:



Chen Hu

Wuhan University

9 PUBLICATIONS 101 CITATIONS

[SEE PROFILE](#)



Jun Xia

Chinese Academy of Sciences

251 PUBLICATIONS 6,790 CITATIONS

[SEE PROFILE](#)



Lingcheng Li

Pacific Northwest National Laboratory

26 PUBLICATIONS 325 CITATIONS

[SEE PROFILE](#)



Zhihong Song

Wuhan University

8 PUBLICATIONS 90 CITATIONS

[SEE PROFILE](#)

Some of the authors of this publication are also working on these related projects:



NGEE-TROPICS [View project](#)



Water ecology and water environment [View project](#)

RESEARCH ARTICLE

A new framework for the identification of flash drought: Multivariable and probabilistic statistic perspectives

Identification of flash drought

Chen Hu^{1,2}  | Jun Xia^{1,2,3} | Dunxian She^{1,2}  | Lingcheng Li⁴ |
Zhihong Song^{1,2} | Si Hong^{1,2}

¹State Key Laboratory of Water Resources and Hydropower Engineering Science, Wuhan University, Wuhan, China

²Hubei Key Laboratory of Water System Science for Sponge City Construction, Wuhan University, Wuhan, China

³Key Laboratory of Water Cycle and Related Land Surface Processes, Institute of Geographic Sciences and Natural Resources Research, Chinese Academy of Sciences, Beijing, China

⁴Atmospheric Sciences and Global Change Division, Pacific Northwest National Laboratory, Richland, Washington

Correspondence

Dunxian She, State Key Laboratory of Water Resources and Hydropower Engineering Science, Wuhan University, Wuhan 430072, P.R. China.
Email: shedunxian@whu.edu.cn

Funding information

the Fundamental Research Funds for the Central Universities, Grant/Award Number: 2042018kf0222; the National Key Research and Development Program of China, Grant/Award Number: 2016YFC0402709; the Strategic Priority Research Program of the Chinese Academy of Sciences, Grant/Award Number: XDA23040304

Abstract

Flash drought is distinguished with seasonal drought by its characteristics of sudden onset and rapid intensification, and has attracted increasing concern due to the severe negative impacts on socioeconomic development and ecosystems. To accurately identify the onset time and propagation of flash drought is still a big challenge, as it is influenced by many factors (e.g., deficit in precipitation, increase in evapotranspiration and temperature, shortage in soil moisture, and etc.). This study aims to develop a probabilistic and multivariable flash drought identification method (PMFDI) from the perspective of considering the interaction effects from different driving factors on flash drought occurrence and propagation with a multivariable statistical tool. The PMFDI uses the weekly standardized precipitation evapotranspiration index and the standardized soil moisture index to describe the abnormally changes in multiple hydrometeorological variables over a short duration. The linearly multivariable index (LMI) is employed to describe the correlation relationship between multiple hydrometeorological variables and to identify flash droughts from the aspects of sudden onset and rapid intensification. We select the Loess Plateau (LP) in China to verify the efficiency of the developed PMFDI with the comparison to the other two recently proposed flash drought identification methods. The results indicate that PMFDI can identify high- and low-frequency regions similar to those identified by the other two methods and can generally recognize actual flash droughts. In addition, the PMFDI can capture the comprehensive impact of multiple hydrometeorological variables as well as their interaction on flash drought occurrence, which provides a useful perspective to understand the propagation processes of the actual flash droughts in the LP.

KEYWORDS

flash drought identification framework, linearly multivariate indicator, precipitation deficit, soil moisture shortage, the Loess Plateau

1 | INTRODUCTION

Traditional drought generally refers to extreme event that persists for an extended time period (mainly several months or years) and can have severe effects on agriculture, ecosystems, socioeconomic activities, water security, and so forth (Mishra and Desai, 2005; She and Xia, 2013; Li, She, *et al.*, 2020). In recent years, flash drought, which is different from traditional droughts mainly due to its sudden onset and rapid intensification, has attracted increasing concern both regionally and globally (Anderson *et al.*, 2013; Otkin, Anderson, Hain, and Svoboda, 2013; Otkin, Anderson, Hain, Mladenova, *et al.*, 2013). Previous studies have indicated that flash droughts are more likely to occur in Northern Hemisphere regions during the crop-growing season (April to September) and can cause severe damage to agricultural production and the environment (Otkin *et al.*, 2018; Christian, Basara, Otkin, and Hunt, 2019; Pendergrass *et al.*, 2020). For example, Jiangxi Province of China suffered flash droughts during the summer of 2003, resulting in direct economic losses from agricultural production of approximately 10 million dollars (Zhang *et al.*, 2017); The flash droughts occurred in the central United States (U.S.) during May–August 2012 caused considerable damage to crops and resulted in billions of dollars in economic losses (Christian, Basara, Otkin, Hunt, Wakefield, *et al.*, 2019). Therefore, the accurate identification of flash droughts can be useful for better understanding the drought formulation mechanism and forecast, which can help formulate drought resistance strategies and reduce the related economic and agricultural losses. It is well known that the accurate definition and identification of the onset and termination time are quite difficult for traditional droughts (Mishra and Singh, 2010; Hao and Aghakouchak, 2013; Li, She, *et al.*, 2020), and similar problems are also faced with flash droughts; this task is still believed to be difficult and needs to be further investigated.

To date, many studies have been dedicated to quantify flash droughts from various aspects. Some studies attempt to quantify flash droughts from the aspect of short duration (Mo and Lettenmaier, 2015, 2016; Wang, Yuan, *et al.*, 2016; Zhang *et al.*, 2017). A representative work is given by Mo and Lettenmaier (2015, 2016), who developed a method to identify flash droughts by detecting abnormalities in multiple hydrometeorological variables, and this method has already been applied in some Northern Hemisphere regions (Mo and Lettenmaier, 2016; Zhang *et al.*, 2017; Wang and Yuan, 2018). However, many studies found that the duration of flash droughts identified by this method is generally no more than 10 days, which is too short to cause damages to local agricultural production (Otkin *et al.*, 2018; Yuan

et al., 2019). In addition, Otkin *et al.* (2018) also indicated that the method proposed by Mo and Lettenmaier (2015, 2016) could not give sufficient quantification of flash drought intensity. Recently, many indices emphasizing the rapid rate of intensification and sudden onset of flash droughts have been proposed and used for detecting flash droughts (Otkin *et al.*, 2016; Koster *et al.*, 2019; Yuan *et al.*, 2019; Christian, Basara, Otkin, Hunt, Wakefield, *et al.*, 2019; Pendergrass *et al.*, 2020). For example, Otkin *et al.* (2016) developed the satellite-derived evaporative stress index to investigate flash droughts in the U.S. during 2012. Koster *et al.* (2019) used the soil moisture percentiles to identify flash droughts in the U.S. and analysed the contributions of different hydrometeorological variables to the occurrence of flash droughts. Christian, Basara, Otkin, Hunt, Wakefield, *et al.* (2019) developed a new flash drought identification method based on the standardized evaporative stress ratio (SESR) and applied it to detect flash droughts in the U.S. Yuan *et al.* (2019) proposed a flash drought identification method based on the soil moisture percentiles and applied it to investigate the flash droughts over China. Pendergrass *et al.* (2020) analysed the physical mechanisms of flash droughts and employed the evaporative demand drought index to identify flash droughts in the U.S. These methods have been shown to be capable of identifying flash droughts.

Many studies have indicated that the occurrence of flash droughts is closely related to anomalies in some hydrometeorological variables, such as precipitation, temperature, evapotranspiration (ET), and soil moisture (Ford and Labosier, 2017; Otkin *et al.*, 2018; Koster *et al.*, 2019; Pendergrass *et al.*, 2020). However, the foregoing flash drought identification methods are usually based on only one or two hydrometeorological variables (Koster *et al.*, 2019; Christian, Basara, Otkin, and Hunt, 2019; Pendergrass *et al.*, 2020). The study that can associate the occurrence of flash drought with the changes in multiple hydrometeorological variables is quite limited. Mo and Lettenmaier (2015, 2016) have attempted to use multiple variables, such as precipitation, ET, and soil moisture, for flash drought detection, but their method cannot quantify the intensity of flash drought (Otkin *et al.*, 2018) and considers little about the interaction among various variables. It arises big interest to develop a method that can couple all these factors together and reflect the comprehensive impact of all possible factors on flash drought propagation. The multivariable tools, which can simultaneously consider the impacts of multiple driving factors on drought occurrence as well as capture the dependence structure between different driving factors (Hao and Aghakouchak, 2013; Hao *et al.*, 2016; She and Xia, 2018), provide a possible way to achieve this goal.

This study proposes a flash drought identification method in a probabilistic way via a multivariable tool (named as PMFDI). The PMFDI involves three steps: (1) characterizing the weekly meteorological and agricultural dry/wet conditions using the standardized precipitation evapotranspiration index (SPEI) (Vicente-Serrano *et al.*, 2010) and the standardized soil moisture index (SSI) (Hao and Aghakouchak, 2013), respectively; (2) characterizing the interactive impact of precipitation, temperature and soil moisture, represented by the weekly SPEI and SSI, on the occurrence of flash droughts using the linearly multivariate index (LMI), first proposed by Hao *et al.* (2016); and (3) identifying flash droughts with suitable criteria that can recognize their sudden onset and rapid intensification. The employed SPEI and SSI in the PMFDI can transfer the hydrometeorological variables into normalized probabilities, which can reflect the dry/wet conditions well and recognize the rapid intensification in droughts (Apurv *et al.*, 2017; González-Hidalgo *et al.*, 2018; Li, She, *et al.*, 2020). The LMI used in the PMFDI is probabilistic and normally distributed and can be used for risk analysis and prediction. In addition, the multivariable structure considered in the PMFDI makes it capable of simultaneously considering multiple variables inducing flash droughts (Hao and Aghakouchak, 2013; Rajsekhar *et al.*, 2015). Two recently developed flash drought identification methods using the similar definition of flash droughts in our study, the method proposed by Christian, Basara, Otkin, and Hunt (2019) using SESR (denoted as SESR method) and the method developed by Yuan *et al.* (2019) using soil moisture percentile (denoted as SMP method), are also employed to provide a comprehensive comparison with the PMFDI. The Loess Plateau (LP) in China is selected as the study area.

The main goals of this study are to: (1) develop a new flash drought identification method on the basis of previous flash drought identification method, the PMFDI, which can simultaneously take multiple hydrometeorological variables as well as their interaction into account via the probabilistic statistical index; (2) evaluate the PMFDI through comparisons with SESR and SMP methods in the LP; and (3) explore the characteristics and trends in the flash droughts that occurred in the LP. The findings of this study can provide scientific support for flash drought identification and prediction and can help mitigate the potential economic losses resulting from flash droughts.

2 | METHOD AND STUDY AREA

2.1 | Methodology

The framework of the PMFDI consists of three steps (Figure 1): (1) the probabilistic transformation of

hydrometeorological variables; (2) the construction of the LMI, and (3) the identification of flash droughts. The SESR and SMP methods are also considered here to evaluate the efficiency of the PMFDI. The specific procedures of these three methods are introduced below.

2.1.1 | Probabilistic and multivariable flash drought identification framework

- i. Probabilistic transformation of hydrometeorological variables

Flash drought is sensitive to precipitation shortages, abnormally high temperatures, and soil moisture deficits (Yuan *et al.*, 2019; Pendergrass *et al.*, 2020), we select SPEI and SSI, which are demonstrated to be applicable on weekly time scale (Nam *et al.*, 2017; Vicente-Serrano *et al.*, 2017; González-Hidalgo *et al.*, 2018), to transform the hydrometeorological variables into normalized variables to better reveal the dry/wet conditions and construct the LMI. The time scale here is selected as weekly because the relatively short time scale can capture the changes in flash droughts (Otkin, Anderson, Hain, Mladenova, *et al.*, 2013; Mo and Lettenmaier, 2016). The SPEI, which can simultaneously identify changes in precipitation and temperature, is constructed with weekly precipitation and potential evapotranspiration (PET) here. The PET is calculated by the Penman-Monteith method as recommended by the Food and Agriculture Organization of the United Nations (Allen *et al.*, 1998). The SSI is calculated with the weekly root-zone (0 ~ 100 cm) soil moisture data and has fewer data requirements than most agricultural drought indices (Hao and Aghakouchak, 2013, 2014; Li, Chen, *et al.*, 2020).

The SPEI and SSI use a similar calculation procedure: selected statistical distributions are used to fit the original data series, which are the difference series between precipitation and PET in the SPEI and the soil moisture series in the SSI, and to obtain the cumulative density function of different levels of the original data series, and then, the inverse normal distribution transformation is used to transform the cumulative density into the standardized values, which can represent different levels of dry/wet conditions. The log-logistic and gamma distributions are adopted as the statistical models in the calculation of SPEI and SSI, respectively (Vicente-Serrano *et al.*, 2010; Hao and Aghakouchak, 2013; Hao *et al.*, 2017).

- ii. Construction of the LMI

The LMI was first proposed by Hao *et al.* (2016) to describe drought conditions from the perspective of multivariable. In the PMFDI, the LMI is adopted as a

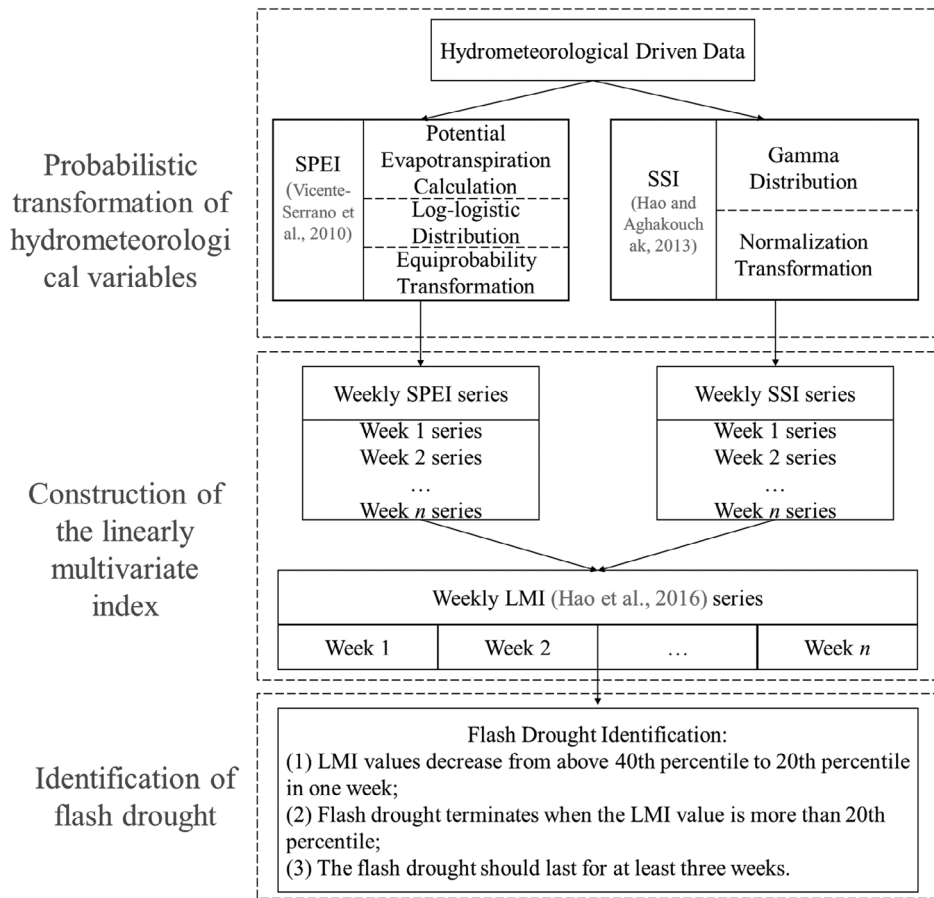


FIGURE 1 Flow chart for the PMFDI

comprehensive drought index to reflect the impacts of multiple hydrometeorological variables on the occurrences of flash droughts. The LMI is constructed under the assumption that the joint distribution of multiple standardized drought indices is a multivariate normal distribution (Hao *et al.*, 2016). The general form of the LMI can be expressed as

$$LMI = \alpha_1 SDI_1 + \alpha_2 SDI_2 + \dots + \alpha_n SDI_n \quad (1)$$

where SDI_n represent different standardized drought indicators (in this case, the SPEI and SSI), which are normally distributed random variables, and $\alpha_1, \alpha_2, \dots, \alpha_n$ are the weights of different indicators. The linear and normally distributed structure of the LMI makes it capable of statistical extrapolation beyond historical observations and simple to construct and apply (She and Xia, 2013; Hao *et al.*, 2016). Based on the theory that a random variable composed of a random vector ($n \times 1$) that follows a multivariate normal distribution can equal a univariate normal random variable (Wilks, 2011), the distribution of the LMI can be considered a normalized distribution with mean u_{LMI} and variance σ_{LMI}^2 . The mean value of the LMI can be expressed as

$$u_{LMI} = \alpha_1 u_1 + \alpha_2 u_2 + \dots + \alpha_n u_n \quad (2)$$

where u_1, \dots, u_n denote the mean values of the standardized drought indicators and are generally close to 0. The variance σ_{LMI}^2 can be calculated as $\alpha^T \Sigma_{LMI} \alpha$ where α^T denotes the vector of the weights $[\alpha_1, \alpha_2, \dots, \alpha_n]$ and Σ_{LMI} denotes the covariance matrix of the LMI as

$$\Sigma_{LMI} = \begin{pmatrix} \text{cov}(SDI_1, SDI_1) & \dots & \text{cov}(SDI_1, SDI_n) \\ \dots & \dots & \dots \\ \text{cov}(SDI_n, SDI_1) & \dots & \text{cov}(SDI_n, SDI_n) \end{pmatrix} \quad (3)$$

The weight vector α^T represents the importance of the different variables in the occurrence of drought event. According to Hao *et al.* (2016), the determination of weights depends on the prior experience or related studies on the importance of different variables to the occurrence of comprehensive drought. The variable with the greatest impact on the occurrence of drought should be assigned the largest weight. As we cannot get sufficient information about the main driving factors of flash droughts in the LP in advance, we assume both precipitation and soil moisture can be considered equally important for the flash droughts in the LP (Yuan *et al.*, 2019;

Pendergrass *et al.*, 2020). So, the weights are set to 0.5 for both the SPEI and SSI for the LP in this study.

iii. Identification of flash drought

In this study, the m weeks during the study period are called as week 1 to M hereafter. The important issue now is the determination of the criteria to characterize flash droughts according to the LMI. The criteria should be determined according to the definition of flash droughts used in this study and can reflect the characteristics of flash droughts, that is, their sudden onset and rapidly increasing intensity and the minimum required length of the duration. Considering some flash drought identification methods that have been applied in China and other countries (Koster *et al.*, 2019; Yuan *et al.*, 2019; Christian, Basara, Otkin, Hunt, Wakefield, *et al.*, 2019), three criteria based on the LMI are proposed to identify flash droughts in this study: (1) the LMI values should decrease from above the 40th percentile to the 20th percentile; (2) the flash drought terminates when the LMI value increases up to the 20th percentile; (3) one flash drought event should last for at least 3 weeks. The first criterion used here is to characterize the rapidly increasing intensity and sudden onset of flash droughts. The 40th and 20th percentiles are widely used as the threshold values of flash drought identification in many previous studies (Ford and Labosier, 2017; Koster *et al.*, 2019; Yuan *et al.*, 2019). The 40th percentile is generally chosen as the threshold values between normal standard and slightly drought, which is used to represent the normal conditions without flash droughts here. The 20th percentile is selected as the threshold value for flash drought occurrences because it is the level at which droughts start to cause damage to crops and pastures and start to have a high risk of fire, according to the associated impacts of different categories of droughts given by the U.S. Drought Monitor (Svoboda *et al.*, 2002). The second criterion is used to define the termination of a flash drought and obtain the complete process of a flash drought event. The third criterion is the minimum required length of the duration for flash droughts and is used to exclude extremely short dry periods, as flash droughts with durations less than 3 weeks are basically insufficient to cause damage to crops and plants in arid regions. In addition, the requirement of the minimum duration of flash droughts is approximately 3 weeks in many previous studies on flash drought identification (Koster *et al.*, 2019; Liu, Zhu, Ren, *et al.*, 2020; Liu, Zhu, Zhang, *et al.*, 2020). These three criteria can guarantee that the identified flash drought has a rapid rate of intensification and can last for a relatively long time to cause damage to agriculture and the environment.

The intensity (I_i) of a flash drought is defined as the average values of the LMI within its duration D_i and is given as:

$$I_i = \frac{1}{D_i} \sum_{j=1}^{D_i} LMI_j \quad (4)$$

2.1.2 | SESR method

The flash drought identification method proposed by Christian, Basara, Otkin, Hunt, Wakefield, *et al.* (2019), which has been used to identify flash droughts in the U.S. (Basara *et al.*, 2019; Christian, Basara, Otkin, and Hunt, 2019; Christian, Basara, Otkin, Hunt, Wakefield, *et al.*, 2019), is employed in this study to evaluate the efficiency of the PMFDI. It is worth noting that the time scale of this method is changed from pentad to week in this study for better comparison with the PMFDI results, so we adapted the minimum required duration of flash drought in this method from 5 or 6 pentads (25 or 30 days) to 4 weeks (28 days). The evaporative stress ratio (ESR) is the basic index for flash drought identification in this method, which is defined as:

$$ESR = \frac{ET}{PET} \quad (5)$$

The SESR and changes in the SESR are defined as:

$$SESR_{ijp} = \frac{ESR_{ijp} - \bar{ESR}_{ijp}}{\sigma_{ESR_{ijp}}} \quad (6)$$

$$(\Delta SESR_{ijp})_z = \frac{\Delta SESR_{ijp} - \bar{\Delta SESR}_{ijp}}{\sigma_{\Delta SESR_{ijp}}} \quad (7)$$

where $SESR_{ijp}$ (referred to as SESR) and $(\Delta SESR_{ijp})_z$ (referred to as $\Delta SESR$) are the z -scores of the ESR and the change in the SESR, respectively. p represents the specific week p , and i and j represent the specific grid point (i, j) . Four criteria involving the SESR are used for flash drought identification: (1) the SESR presents a negative trend for at least 4 weeks; (2) the final value of the SESR is less than the 20th percentile; (3) the week-to-week changes in the SESR ($\Delta SESR$) are not greater than 40th percentile; (4) the changes in the SESR over the entire flash drought event should be less than 25th percentile. The first two restrictive criteria emphasize the rapid rate of flash drought intensification, and the other criteria focus on the impacts on vegetation (Christian, Basara, Otkin, Hunt, Wakefield, *et al.*, 2019).

2.1.3 | SMP method

Here, the flash drought identification method proposed by Yuan *et al.* (2019), which has been used for flash drought identification for the whole of China, is also adopted in this study. Similar to the adaptations in SESR method, the time scale is also set to week instead of pentad here. Thus, the minimum requirement of the flash drought duration in this method is changed from 3 pentads (15 days) to 2 weeks (14 days). Weekly mean root-zone (0–100 cm) soil moisture data are used in this method for flash drought identification. A flash drought is identified when it satisfies the following requirements: the soil moisture decreases from above the 40th percentile to the 20th percentile, and the average decreasing rate is no less than 5% in percentile for each week; the flash drought terminates if the soil moisture level is greater than the 20th percentile; and the flash drought should last for at least 2 weeks.

For these three methods, the frequency of occurrence (FOC) for each pixel is defined as the percentage of weeks under flash drought conditions.

$$\text{FOC} = 100\% \times N_{FD} / N_{total} \quad (8)$$

where N_{total} is the total number of weeks and N_{FD} is the number of weeks associated with flash droughts.

2.2 | Study area and data

The Loess Plateau (33.72–41.27°N, 100.09–114.55°E), which traverses the upper-middle reaches of the Yellow River in China, is not only the largest loess region in China but is also well known for its severe soil erosion and water shortages. This region covers an area of approximately 640,000 km² and includes Shaanxi Province, Shanxi Province, the Ningxia Autonomous Region, some eastern areas of Qinghai Province, central and eastern Gansu Province, some northern areas of Henan Province, and some southern areas of the Inner Mongolia Autonomous Region. The elevation of the LP varies from 4,950 m in the west to 78 m in the east. The LP features a continental monsoon climate region, and the mean annual temperature in this region ranges from 4°C to 14°C. The long-term annual mean precipitation ranges from 200 mm in the northwest to 800 mm in the southeast (Wang *et al.*, 2010; She and Xia, 2018), and most precipitation events occur from June to September (Zhang *et al.*, 2012). The annual mean PET in the LP is estimated to be much higher than the annual mean precipitation, and ranges from 865 mm to 1,274 mm (Wu *et al.*, 2018). The specific location and geographical information of the LP can be found in Figure 2.

In this study, the daily precipitation, near-surface temperature, wind speed, humidity, pressure, root-zone (0 ~ 100 cm) soil moisture, and ET data from 1979 to 2014 with a horizontal resolution of 0.25° × 0.25° are employed for the identification of flash droughts. The daily root-zone soil moisture and ET data are acquired from the Global Land Data Assimilation System (GLDAS) version 2.0 Catchment Land Surface Model (CLSM) dataset (<https://disc.gsfc.nasa.gov/datasets>) (Rodell *et al.*, 2004; Li *et al.*, 2018). This dataset is simulated from the Catchment Land Surface Model 3.3 and contains a long-term series (from January 1948 to December 2014) of land parameters with a spatial resolution of 0.25° × 0.25°. The input data of the GLDAS CLSM dataset come from the Princeton meteorological forcing dataset, which is constructed by bias correcting the precipitation, solar radiation, and air temperature observation and reanalysis data from the National Center for Environmental Prediction (NCEP)/National Center for Atmospheric Research (NCAR) (Sheffield *et al.*, 2006; Xia *et al.*, 2019). The accuracy of the GLDAS ET and soil moisture data in some northern areas of China has been evaluated by some studies through comparisons with observation data or other reanalysis datasets (Zhu and Shi, 2014; Wang, Cui, *et al.*, 2016; Bai and Liu, 2018). The precipitation, near-surface temperature, wind speed, humidity, and pressure are obtained from the China Meteorological Forcing Dataset (CMFD), which is developed by the Institute of Tibetan Plateau Research, Chinese Academy of Sciences (<http://www.tpdc.ac.cn/zh-hans/data/8028b944-daaa-4511-8769-965612652c49/>) (Yang *et al.*, 2010; Yang and He, 2018; He *et al.*, 2020). The CMFD covers the region within 15–55°N, 70–140°E and has a long time period (1979–2018) with a spatial and temporal resolution of 0.1° × 0.1° and 3 hr, respectively. This dataset contains precipitation, downward shortwave radiation, downward longwave radiation, 2 m air temperature, humidity, wind speed and surface pressure data. This product was made through the fusion of ground-based observations and gridded reanalysis/remote sensing datasets. More specific information about the CMFD can be found in the study of He *et al.* (2020). Many studies have evaluated the accuracy of the CMFD by comparing it with observation data or other reanalysis datasets (Chen *et al.*, 2011; Wang *et al.*, 2017; Yang *et al.*, 2017; Li, She, *et al.*, 2020).

In this study, according to the climatic conditions and crop growing situation in the LP, only weeks from April first to September 30th (26 weeks per year) are analysed, so there are a total of 936 weeks in the 36-year record from 1979 to 2014. The CMFD product is resampled to the same spatial resolution as the GLDAS CLSM dataset, and the weekly

FIGURE 2 The map of the LP. The underlined and italic fonts represent the names of corresponding provinces or autonomous regions [Colour figure can be viewed at wileyonlinelibrary.com]

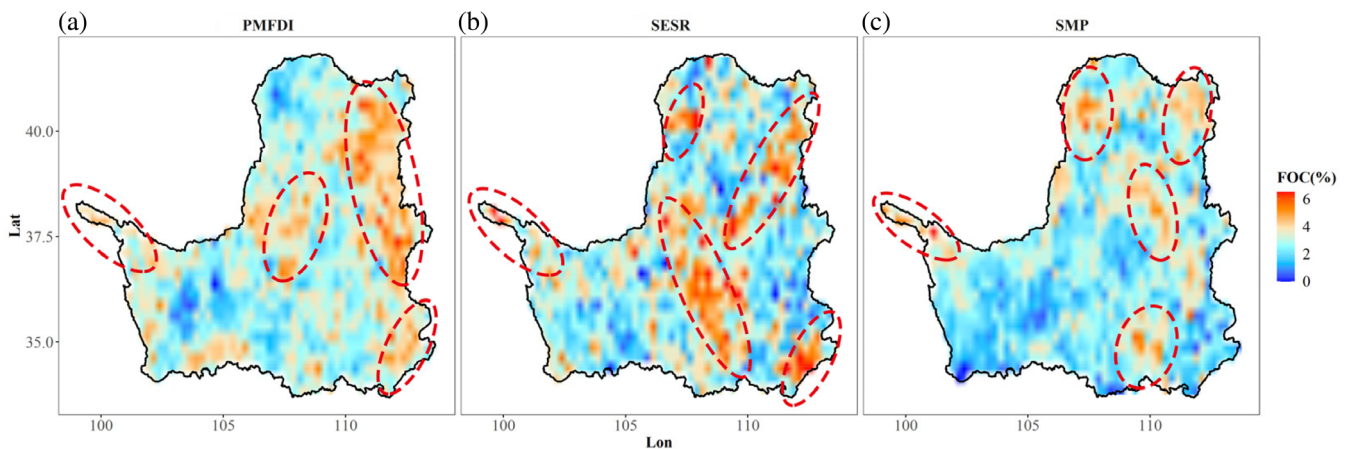
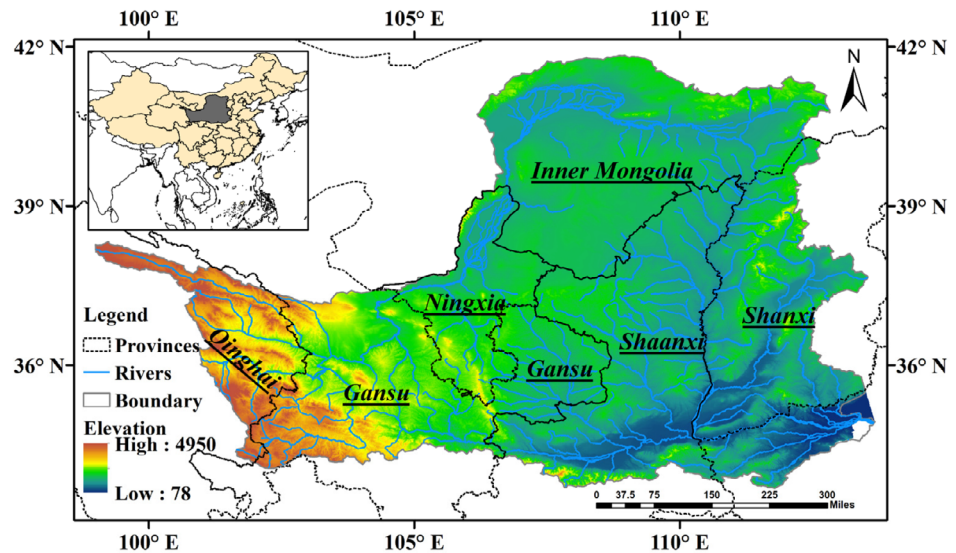


FIGURE 3 The frequency of occurrences of weeks under the flash droughts identified by (a) PMFDI, (b) SESR method, and (c) SMP method. The dotted circles denote the high flash drought frequency regions [Colour figure can be viewed at wileyonlinelibrary.com]

hydrometeorological data are derived from the corresponding gridded datasets.

3 | RESULTS

3.1 | Frequency of flash droughts identified by three methods

Based on the weekly precipitation, PET, and root-zone soil moisture data from April to September from 1979 to 2014, the weekly SPEI and SSI series of 26 weeks are computed for the whole LP, and the LMI series for each week are constructed with the corresponding SPEI and SSI series. The flash droughts in the whole LP from 1979 to 2014 are identified by PMFDI, SESR, and SMP, respectively. A similar range of FOC of flash droughts can be identified by the three methods (Figure 3). The results of

the PMFDI in Figure 3 (a) indicate that the regions with high FOC are mainly located in the far northwestern, central and eastern LP, while the low frequency regions are generally located in the western and northern LP. In addition, most areas in the far northwestern, far northeastern and southeastern LP are also recognized as high FOC regions by SESR and SMP methods as indicated in Figure 3(b) and (c). Moreover, most western areas of LP are identified as the low FOC regions by all three methods. The similar results in three methods indicate that PMFDI can identify some similar high and low FOC regions as the other two methods.

However, there also exists some differences in FOC spatial pattern of three methods. For example, the south-central LP is identified as the high FOC region by SESR method, but it is identified as a relatively low FOC region by PMFDI and SMP method. Such a difference may be caused by the different consideration to flash drought

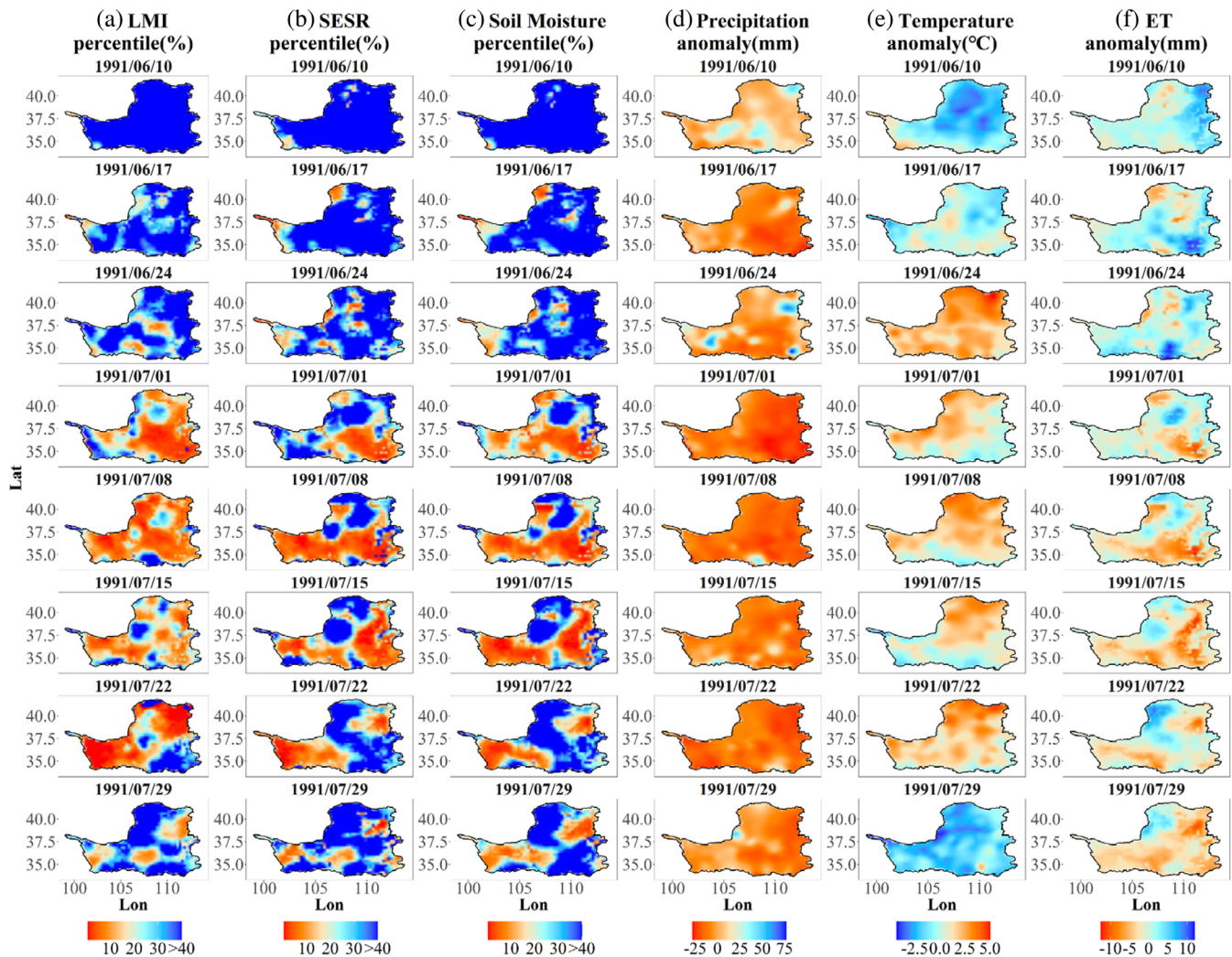


FIGURE 4 The weekly evolutions of (a) LMI percentile (%), (b) SESR percentile (%), (c) soil moisture percentile (%), (d) precipitation anomaly (mm), (e) temperature anomaly ($^{\circ}\text{C}$), and (f) ET anomaly (mm) in the 1991 flash drought event. The dates (in the form of year/month/day) above each figure represent the onset time of this week (June 10, 1991 means the period from June 10, 1991 to June 16, 1991) [Colour figure can be viewed at wileyonlinelibrary.com]

inducing factors in the three methods and the effect of precipitation. As shown in Figure S1, the precipitation amount is higher in the southwestern areas than the northwestern areas. The relatively abundant precipitation may replenish the soil water at the high rate of ET and reduces the rate of soil moisture loss. Thus, the frequency of flash droughts identified by the PMFDI and SMP method may be lower in this region since both methods consider the impact of the soil moisture on the occurrence of flash droughts. Such results also indicate that different flash drought identification methods may affect the FOC results to some extent. In addition, the FOC results of PMFDI are generally consistent with the results in the study of Liu, Zhu, Ren, *et al.* (2020), who found that high FOC regions in the LP are mainly located in the northern and southeastern regions.

3.2 | Typical flash drought events identification

Two typical flash drought events are selected to explore the performance of PMFDI in flash drought event tracking. The first one is the 1991 flash drought event provided in the study of Liu, Zhu, Ren, *et al.* (2020), which occurred from June 11th to July 23rd in 1991. Figure 4 provides the weekly evolutions of the LMI, SESR, soil moisture, as well as some hydrometeorological variables during this flash drought event. For convenience, we use the combination of the week and date to indicate the week starting from this date hereafter. For example, week June 24th represents the week starting from June 24th to June 30th. Figure 4 indicates that the western and central areas present a quickly decreasing trend in LMI values

from higher than 40th percentile to lower than 20th percentile in week June 24th. Such decreasing trends in LMI values can also be found in the southern and northern areas in the week July first. This result implies the migration and propagation processing of this flash drought event from the western and central LP to the southern and northern LP, which is consistent with Liu, Zhu, Ren, *et al.* (2020). In addition, considering all criteria in the SESR and SMP methods, the evolutions of SESR and soil moisture in these weeks indicate the similar flash drought propagation processing, which means that all three methods can generally capture the evolution of this flash drought event. Figure 4 also displays the changes in the anomalies of some hydrometeorological variables. As shown in Figure 4(d) and (e), the precipitation anomalies are all negative, and the temperature anomalies rapidly increase from negative values to positive values in week June 24th. In addition, the soil moisture in some regions also experience a sharp decrease in week June 24th, and such a decrease in soil moisture is more obvious for many regions in week July first. This result indicates that the precipitation deficit and abnormally high temperature may be closely related to the soil moisture shortage. In addition, the ET anomalies are higher than zero in the first 3 weeks but has been in the negative values since week July first. As suggested by Liu, Zhu, Zhang, *et al.* (2020) and Koster *et al.* (2019), the weekly evolution of ET anomaly in this flash drought implies that the increase in ET at the beginning of flash drought may be related to the rapidly increasing temperature. The changes of these hydrometeorological variables are also consistent with the results in the study of Liu, Zhu, Ren, *et al.* (2020), though their study used different datasets.

Another selected flash drought was the 1997 flash drought occurred in the Gansu province (the western areas and some central areas of LP, see Figure 2) from August first to September 30th in 1997. It caused approximately 1.48×10^6 ton grain losses to the Gansu province as recorded in the studies of Deng *et al.* (2007) and Ren *et al.* (2013). The specific weekly evolutions of some key variables are given in Figure 5. Figure 5 shows that the LMI, SESR, and soil moisture in the central LP both rapidly decrease from high values to low values in week August ninth, and such decreasing trends can be further detected in the western LP in week August 16th, which indicates that this flash drought have spread from the central LP to the western LP. The migration and evolutions of LMI, SESR, and soil moisture indicate that the three methods can both identify this flash drought event occurred in the western and central LP. However, there is still some differences in the spatial patterns of LMI, SESR, and soil moisture during the 1997 flash drought. In week August 23rd, most areas in the Gansu province

may be affected by this flash drought event as recorded in the literature (Deng *et al.*, 2007; Ren *et al.*, 2013). Figure 5 illustrates that in this week, the LMI values in most western and central areas are less than 20th percentile, while the SESR and soil moisture values in most of these areas are higher than 20th percentile. In addition, Figure 5(d) and (e) also indicate that in week August 23rd, the precipitation and temperature anomalies in most central and western areas are in the negative and positive values, respectively. This implies that the LMI may response more rapidly to the abnormally changes in hydrometeorological variables compare to SESR and soil moisture. This rapid response in the LMI is likely due the combined effects of incorporating precipitation deficits with abnormally high surface temperatures and a shortage in soil moisture. While SESR and SMP method indirectly incorporate impacts associated with a lack of precipitation, the inclusion of precipitation deficits directly in the LMI may allow the LMI to respond more quickly at the beginning of flash drought development. Thus, the performance evaluation of PMFDI on FOC identification and typical flash droughts tracking indicates that the PMFDI has the ability to identify flash droughts in the LP.

3.3 | Characteristics of flash droughts in the LP

The average duration of the flash droughts identified by the PMFDI for the entire LP over the period from 1979 to 2014 are displayed in Figure 6 (a). It can be found that the average durations of the flash droughts range from 3 to 7 weeks, and the flash droughts that occurred in the southern areas generally have longer durations than those in the northern LP. The intensity of each flash drought can be calculated via Equation (4), and the spatial distribution of the average intensity of flash droughts identified by the PMFDI is presented in Figure 6(b). The regions with high flash drought intensity are mainly located in the western areas and some southern areas. In addition, the flash drought intensity presents an increasing trend from the east to the west. The total duration of the flash droughts occurred in each calendar month for each pixel during the period from 1979 to 2014 is accumulated, and then the regional average value of the total durations of flash droughts of all pixels is calculated for each calendar month and displayed in Figure 7. The regional multiple-year average duration of flash droughts occurred in each calendar month vary from 1.66 to 7.07 weeks. August has the largest cumulative number of weeks under flash drought, followed by May and July, while September has the smallest cumulative number of

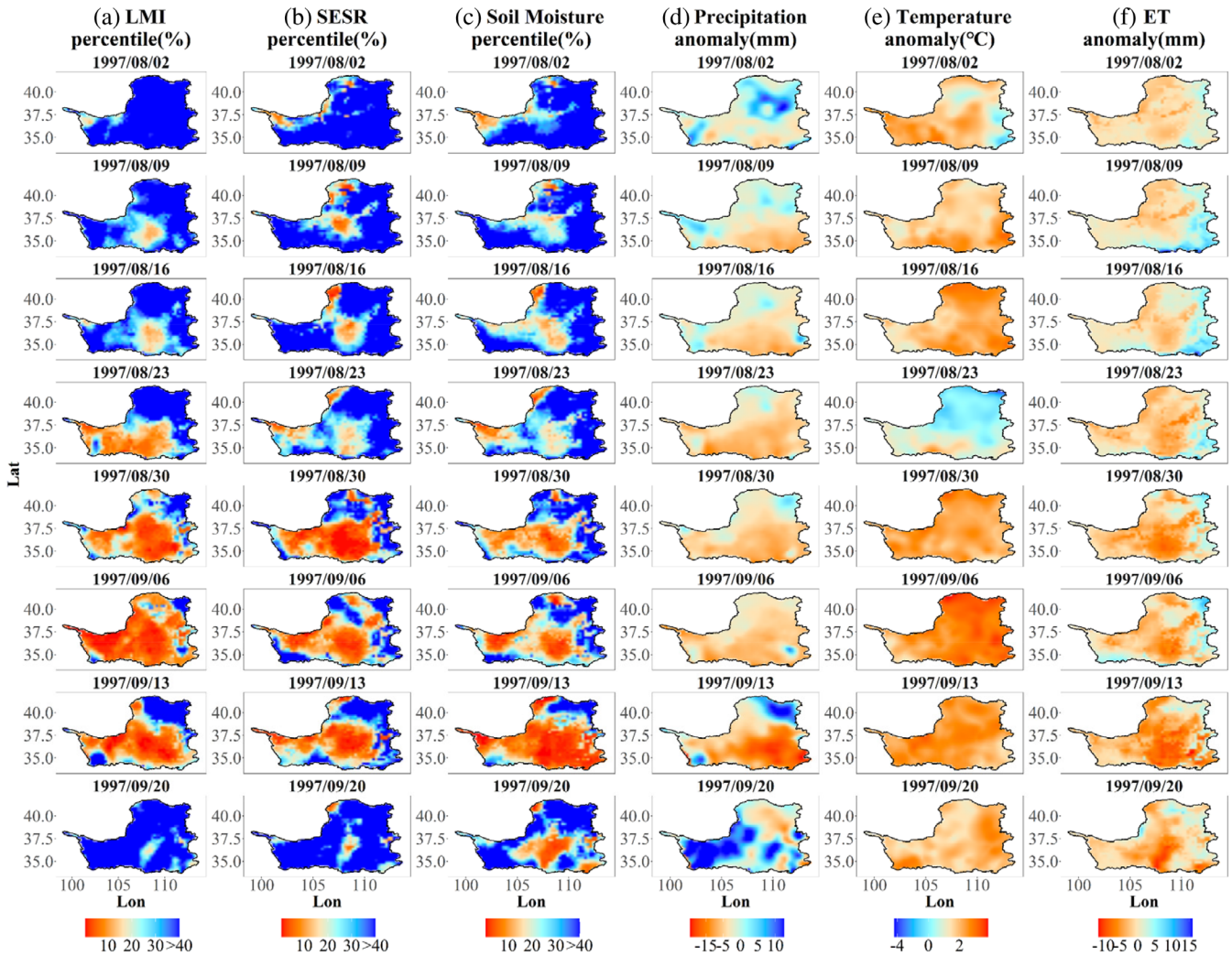


FIGURE 5 The weekly evolutions of (a) LMI percentile (%), (b) SESR percentile (%), (c) soil moisture percentile (%), (d) precipitation anomaly (mm), (e) temperature anomaly (°C), and (f) ET anomaly (mm) in the 1997 flash drought event [Colour figure can be viewed at wileyonlinelibrary.com]

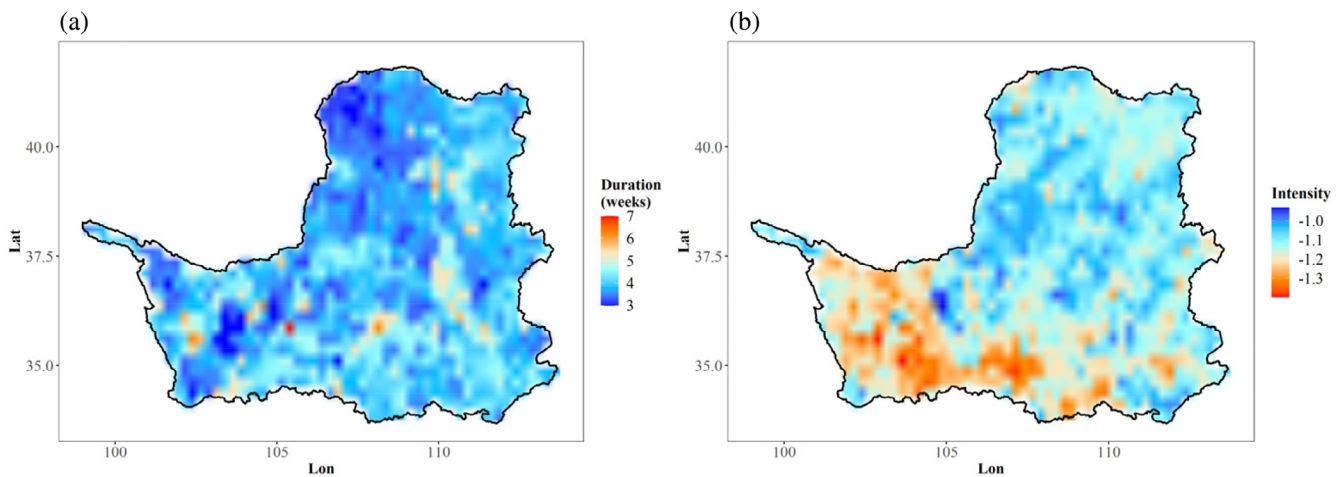


FIGURE 6 The spatial distribution of multiyear averaged duration (a) and intensity (b) of the flash droughts identified by PMFDI in the LP during 1979–2014 (the smaller value in (b) indicates the higher intensity of flash drought) [Colour figure can be viewed at wileyonlinelibrary.com]

weeks under flash drought. The low regional average durations of flash droughts that occurred in September and some months are caused by a large number of pixels with no flash droughts identified in these months.

Figure 8 presents boxplots of precipitation anomalies, temperature anomalies, and soil moisture percentiles 1 week prior to onset, at onset, and 1 week after the end of all the flash droughts identified by the PMFDI. The changes in precipitation, temperature, and soil moisture demonstrate the effects of flash droughts on the hydro-meteorological variables. Compared to 1 week before the onset of the flash droughts, the average values of the precipitation anomalies and soil moisture percentiles both present decreasing trends, and the average values of the temperature anomalies show increasing trends when flash droughts occur. In addition, the mean values of the precipitation and temperature anomalies both recover to values close to zero, and the mean soil moisture percentiles increase to relatively high values when the flash

droughts terminate. The changes in precipitation, temperature, and soil moisture demonstrate that the flash droughts identified by the PMFDI have impacts on the local hydrometeorological variables, which is consistent with the definition of flash droughts and the findings of other flash drought identification methods (Mo and Lettenmaier, 2015; Yuan *et al.*, 2019; Pendergrass *et al.*, 2020).

3.4 | Trends in the flash droughts in the LP

The average number of weeks with flash droughts identified by the PMFDI per year over the entire LP is given in Figure 9 to explore the interannual variability in the flash droughts. The figure shows that there are more than 2 weeks with flash droughts in 1994, 1997, and 2001, while 1997 had the largest number of weeks with flash droughts. The mean number of weeks with flash droughts exhibits an increasing trend from 1979 to 2014, while this increasing trend is not significant. To further investigate the trends in the number of weeks under flash drought from 1979 to 2014 over the entire LP, we run the Mann–Kendall (MK) test (Mann, 1945; Forthofer and Lehnen, 1981) on the annual flash drought number series for each pixel (Figure 10). Most southern areas and some northeastern areas present increasing trends in the number of flash droughts, while the regions with decreasing trends are mainly located in some northern and western areas of the LP. Furthermore, we also apply the MK test to the annual mean precipitation, temperature, and root-zone soil moisture to detect their trends over the period from 1979 to 2014 (Figure 11). The precipitation presents increasing trends in most areas, especially in the western and central LP. Only some southern areas show decreasing trends in precipitation. Figure 11(b) shows that most areas of the LP present

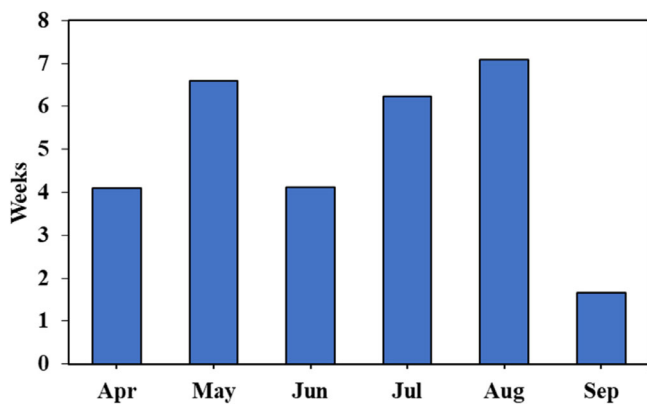


FIGURE 7 The cumulative number of weeks with flash droughts identified by PMFDI for each month averaged over the LP from 1979 to 2014 [Colour figure can be viewed at wileyonlinelibrary.com]

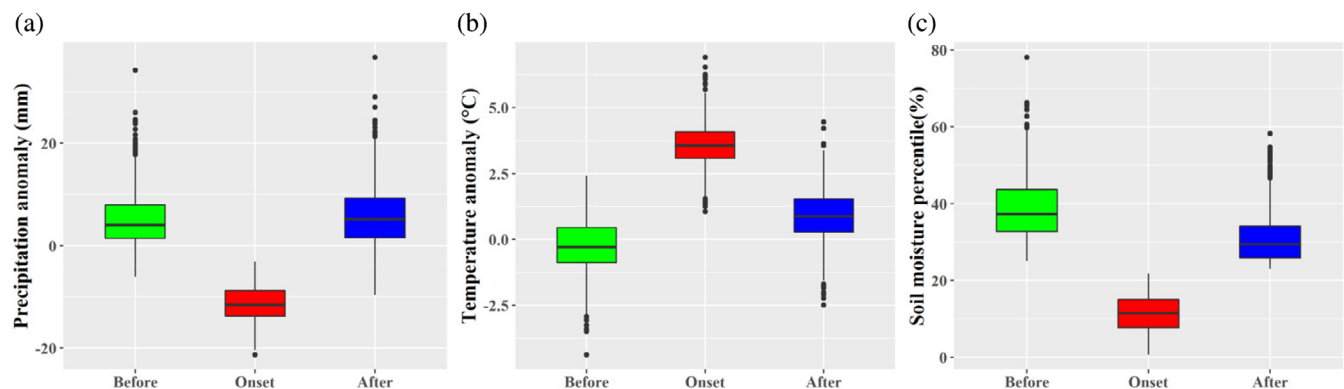


FIGURE 8 The boxplots of the precipitation anomaly (a), temperature anomaly (b), and soil moisture percentile (c) 1 week prior to onset, at onset, and 1 week after the end of all flash droughts identified by PMFDI [Colour figure can be viewed at wileyonlinelibrary.com]

significant increasing trends in temperature. Figure 11(c) shows that the soil moisture in the southern and western LP has decreased and increased, respectively. The spatial patterns of the key factors inducing flash droughts in Figure 11 show some connections with the results in Figure 11. Most areas in the southern LP show decreasing trends in both precipitation and soil moisture but increasing trend in the number of weeks with flash droughts. Similarly, most areas in the western LP present decreasing trends in the number of weeks with flash droughts, while increasing trends in precipitation and soil moisture are detected in these regions.

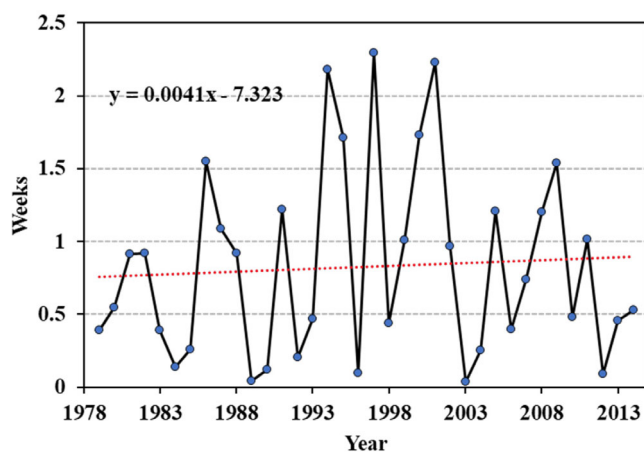


FIGURE 9 The number of weeks with flash drought identified by PMFDI per year averaged over the entire LP from 1979 to 2014; the red dashed line indicates the trend of the number of weeks [Colour figure can be viewed at wileyonlinelibrary.com]

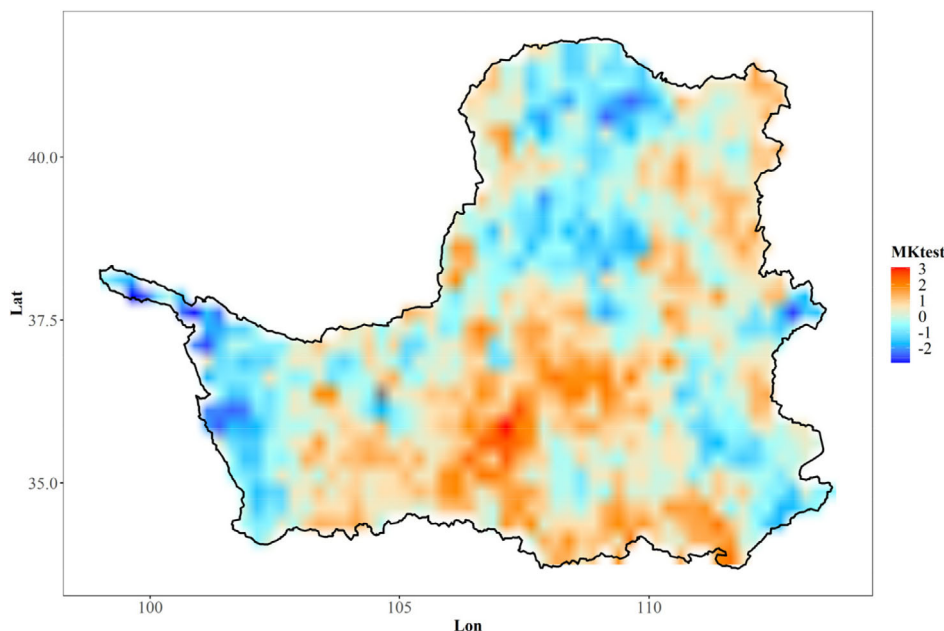


FIGURE 10 The spatial pattern of the Mann-Kendall test results for the weeks with flash droughts identified by PMFDI over the period of 1979–2014 [Colour figure can be viewed at wileyonlinelibrary.com]

4 | DISCUSSION

4.1 | Comparisons of the three flash drought identification methods

In this study, we propose the PMFDI to identify flash droughts in a probabilistic way via a multivariable tool (i.e., the LMI). Another two recently developed methods, SESR, and SMP methods, are also employed to evaluate the efficiency of the PMFDI in flash drought identification. The evaluation results show that the PMFDI can identify some similar high frequency and low regions as other two methods, while the high frequency regions are generally consistent with the study of Liu, Zhu, Ren, *et al.* (2020). Our results also indicate that the three methods can basically capture the migration and propagation of two flash drought events occurred in 1991 and 1997, which demonstrates the applicability of the PMFDI in flash droughts tracking.

As indicated by many studies (Mo and Lettenmaier, 2016; Otkin *et al.*, 2018; Koster *et al.*, 2019; Pendergrass *et al.*, 2020), anomalies in various hydrometeorological variables will largely alter the water cycle and land-atmosphere feedback in specific regions and thus induce flash droughts. For example, precipitation shortages, above-average temperatures, rapid decreases in soil moisture, or the comprehensive effects of these variables both have the potential to trigger flash droughts. Precipitation deficit may lead to an insufficient water supply for plants and water bodies and cause soil aridity and plant wilt. Abnormally high temperature can lead to a rapid increase in ET, which can accelerate the decrease in soil moisture and ground water levels. A rapid decrease in the soil moisture can cause crops to wither and even die. Simultaneous abnormal changes in

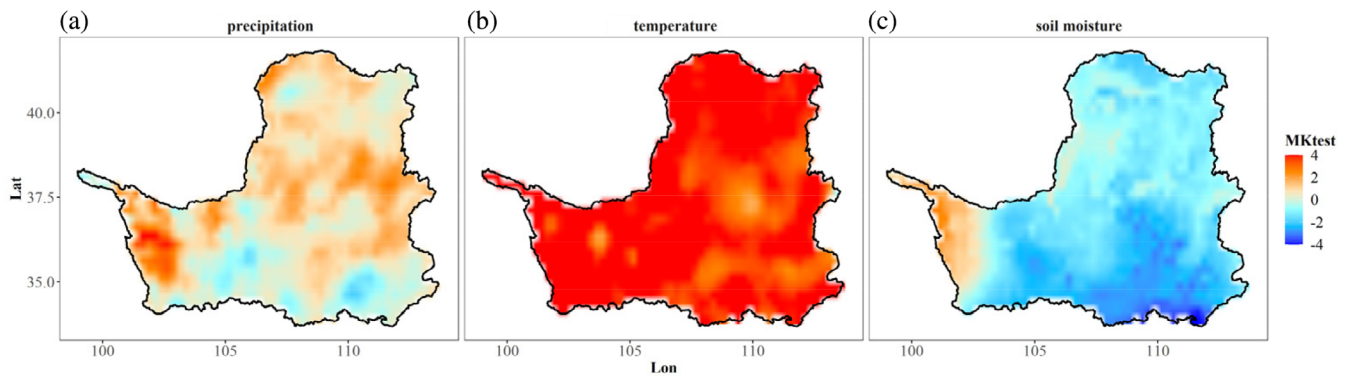


FIGURE 11 The spatial pattern of the Mann-Kendall test results for precipitation (a), temperature (b), and root zone soil moisture (c) over the period of 1979–2014 [Colour figure can be viewed at wileyonlinelibrary.com]

multiple variables have the potential to trigger or exacerbate flash droughts (Pendergrass *et al.*, 2020). The advantages of the PMFDI mainly lie in that it can simultaneously consider different variables inducing flash droughts as well as their interaction and give a comprehensive judgement of abnormalities in multiple variables. Most current flash drought identification methods ignore the interaction between multiple variables or only consider the effects of one or two variables on the occurrence of flash drought, which may be less accurate for the regions with complicated hydrometeorological conditions. The LMI used in the PMFDI can simultaneously consider changes in precipitation, temperature, and soil moisture in the identification of flash droughts, which are the main hydrometeorological driving factors of flash droughts (Ford *et al.*, 2015; Otkin *et al.*, 2018). Thus, the LMI can be considered a comprehensive result of multiple variables, which can provide a comprehensive judgement based on the changes in various hydrometeorological variables. As indicated in Figure 4 and Figure 5, the regions with significant changes in LMI are generally consistent with the regions where precipitation, temperature and soil moisture are both at the abnormal levels. In addition, the LP is a well-known arid region experiencing severe soil erosion and water shortages (Liu *et al.*, 2016). The droughts here are sensitive to changes in both precipitation and soil moisture and can be altered by the comprehensive influence of multiple hydrometeorological variables (Wang *et al.*, 2015; Liu *et al.*, 2016). The basic theory of the PMFDI makes it more suitable to illustrate the comprehensive impacts of multiple variables on the occurrence of flash drought in the LP.

4.2 | Possible interaction between flash droughts and vegetation in the LP

In the past several decades, the vegetation conditions in the study area have largely changed by the applied Grain

to Green Program (GGP) in the central areas of the LP since 1999, which aimed to change the agricultural areas into grassland and forestland and to increase the amount of vegetation cover in the region (Feng *et al.*, 2016; Wang *et al.*, 2018; Zhang *et al.*, 2018). Zhao *et al.* (2019) indicated that the normalized difference vegetation index (NDVI) showed a significant increasing trend of 0.0042 per year for the whole LP from 2000 to 2014, which implied an increase in the amount of vegetation in the LP. However, a decreasing trend in the soil moisture and an increasing trend in droughts have been detected in the LP since 2000 (Liang *et al.*, 2018; Zhao *et al.*, 2019). The interaction and feedback between droughts, including flash droughts, and vegetation are quite complex. On the one hand, the occurrence of flash droughts, which is generally accompanied by precipitation deficits, high temperatures or soil moisture shortages, will have negative impacts on the growth of plants. On the other hand, the frequency of flash droughts can be influenced by the land use types. Figure 4 shows that the flash drought frequency is lower in the central LP than in the northwestern LP, while most agricultural areas in the central LP changed into grassland and forestland because of the GGP. As indicated by Christian, Basara, Otkin, Hunt, Wakefield, *et al.* (2019), the possible reason for this result may be that compared to grassland and forestland, the flash drought frequency may be higher in the agricultural regions because of a shallower root zone and a higher rate of ET.

4.3 | Uncertainties in the PMFDI

There are still some uncertainty issues in the PMFDI that deserve further discussion. One of these factors is the influence of different time scales on the PMFDI results. In this study, weekly data are employed in the PMFDI, as this is the acceptable time scale of the SPEI suggested by

Vicente-Serrano *et al.* (2017) and González-Hidalgo *et al.* (2018). The time scales of SESR method and SMP method are both adapted from pentad to week, which may cause some negative impacts on the results of these two methods. However, as there is no evidence that the SPEI and SSI can be applied on the pentad time scale, the coarsening of the time scale of SESR method and SMP method seems to be the only way to make the time scale of the three methods the same. The feasibility of using a smaller time scale in the PMFDI remains to be further verified. Another issue that may create uncertainty in the PMFDI results is the selection of the statistical distributions in the SPEI and SSI. In this study, we select the log-logistic and gamma distributions, respectively, among many statistical distributions (gamma, log-logistic, log-normal, general extreme value, and Pearson-III distributions) widely used in the calculation of standardized drought indices (Mishra and Desai, 2005; Mishra and Singh, 2010; Vicente-Serrano *et al.*, 2010) for the calculations of the SPEI and SSI in the LP, respectively, while their applicability on weekly SPEI and SSI calculation has also been evaluated by comparing with some other distributions (Table S1). However, the best choices for the frequency distributions used in the PMFDI may be different in other regions, and different choices for the frequency distributions will greatly impact the results of the SPEI, SSI, and even the PMFDI. In addition, similar to many previous studies (Yuan *et al.*, 2019; Christian, Basara, Otkin, Hunt, Wakefield, *et al.*, 2019; Pendergrass *et al.*, 2020), reanalysis datasets, which are developed by running large-scale models and data assimilation systems, are used to identify flash droughts. Therefore, the accuracy of these reanalysis datasets will probably influence the efficiency of flash drought identification. The bias in the reanalysis datasets will have some negative impact on the efficiency of the flash drought identification results.

5 | SUMMARY AND CONCLUSION

In this study, we propose a framework to identify flash droughts, named the PMFDI. The PMFDI is applied for the identification of flash droughts during the growing season (April to September) in the LP with the weekly hydrometeorological data from 1979 to 2014. Two flash drought identification methods, which were proposed by Christian, Basara, Otkin, Hunt, Wakefield, *et al.* (2019) and Yuan *et al.* (2019), are employed to evaluate the effectiveness and efficiency of the PMFDI in flash drought identification. The spatiotemporal characteristics, as well as the trends in the flash droughts on the LP, are also investigated and analysed in detail in this study. The main conclusions of this study are as follows:

(1) The three methods can both identify the high frequency flash drought regions are mainly located in the far northwestern and eastern areas of the LP, while most western areas of LP are identified as the low frequency flash drought regions by all three methods. In addition, the three methods can both identify the 1991 and 1997 flash drought events in the LP well. The results above demonstrate that the acceptable performance of PMFDI in flash drought frequency identification and typical flash drought tracking. Moreover, the weekly evolutions of key hydrometeorological variables in the two typical flash drought events also indicate that PMFDI can give a comprehensive judgement based on multiple variables compared to SESR and SMP methods.

(2) The spatial distributions of the average severity and duration of flash droughts show that some western areas have shorter durations and higher intensity than other areas. The monthly characteristics of the flash droughts show that the monthly cumulative number of weeks under flash drought is highest in August and lowest in September.

(3) The trend analysis of the number of weeks under flash droughts shows that the regions with increasing trends in the number of flash droughts are located in most southern areas and some northeastern areas, while the regions with decreasing trends are mainly located in some northern and western areas of the LP. The mean number of weeks with flash droughts presents an increasing trend from 1979 to 2014, which indicates the risk of flash droughts with long durations in the future. The precipitation, temperature, and soil moisture trend analysis indicate that the trends in the three variables are related to the trends in the flash droughts in the LP.

ACKNOWLEDGEMENTS

This study was financially supported by the National Key Research and Development Program of China (2016YFC0402709), the Strategic Priority Research Program of the Chinese Academy of Sciences (grant no. XDA23040304) and the Fundamental Research Funds for the Central Universities (grant no. 2042018kf0222). The hydrometeorological data used in this study were collected from the GLDAS_CLSM025_D_2.0 dataset and the Data Assimilation and Modelling Center for Tibetan Multi-spheres, Institute of Tibetan Plateau Research, Chinese Academy of Sciences, which were highly appreciated.

ORCID

Chen Hu  <https://orcid.org/0000-0002-6454-3739>

Dunxian She  <https://orcid.org/0000-0003-4660-3301>

REFERENCE

Allen, R.G., Pereira, L.S., Raes, D. and Smith, M. (1998) *Crop Evapotranspiration-Guidelines for Computing Crop Water*

- Requirements-FAO Irrigation and Drainage Paper 56*. Rome: FAO.
- Anderson, M.C., Hain, C., Otkin, J., Zhan, X., Mo, K., Svoboda, M., Wardlow, B. and Pimstein, A. (2013) An Intercomparison of drought indicators based on thermal remote sensing and NLDAS-2 simulations with U.S. drought monitor classifications. *Journal of Hydrometeorology*, 14, 1035–1056. <https://doi.org/10.1175/JHM-D-12-0140.1>.
- Apurv, T., Sivapalan, M. and Cai, X. (2017) Understanding the role of climate characteristics in drought propagation. *Water Resources Research*, 53, 9304–9329. <https://doi.org/10.1002/2017WR021445>.
- Bai, P. and Liu, X. (2018) Intercomparison and evaluation of three global high-resolution evapotranspiration products across China. *Journal of Hydrology*, 566, 743–755. <https://doi.org/10.1016/j.jhydrol.2018.09.065>.
- Basara, J.B., Christian, J.I., Wakefield, R.A., Otkin, J.A., Hunt, E. and Brown, D.P. (2019) The evolution, propagation, and spread of flash drought in the Central United States during 2012. *Environmental Research Letters*, 14, 14. <https://doi.org/10.1088/1748-9326/ab2cc0>.
- Chen, Y., Yang, K., He, J., Qin, J., Shi, J., Du, J., and He, Q. (2011) Improving land surface temperature modeling for dry land of China. *Journal of Geophysical Research*, 116(D20). <http://doi.org/10.1029/2011jd015921>.
- Christian, J.I., Basara, J.B., Otkin, J.A. and Hunt, E.D. (2019a) Regional characteristics of flash droughts across the United States. *Environmental Research Communications*, 1, 125004. <https://doi.org/10.1088/2515-7620/ab50ca>.
- Christian, J.I., Basara, J.B., Otkin, J.A., Hunt, E.D., Wakefield, R.A., Flanagan, P.X. and Xiao, X. (2019) A methodology for flash drought identification: application of flash drought frequency across the United States. *Journal of Hydrometeorology*, 20, 833–846. <https://doi.org/10.1175/jhm-d-18-0198.1>.
- Deng, Z., Zhang, Y., Liu, D., Mao, Y., Qin, Z., Xue, W., Zhao, H. and Yuan, Z. (2007) Study on influence of arid climate change to drought disaster in Gansu and technique of preventing drought and reducing disaster (in Chinese). *Agricultural Research in the Arid Areas*, 25, 94–99.
- Feng, X., Fu, B., Piao, S., Wang, S., Ciais, P., Zeng, Z., Lü, Y., Zeng, Y., Li, Y., Jiang, X. and Wu, B. (2016) Revegetation in China's loess plateau is approaching sustainable water resource limits. *Nature Climate Change*, 6, 1019–1022. <https://doi.org/10.1038/nclimate3092>.
- Ford, T.W. and Labosier, C.F. (2017) Meteorological conditions associated with the onset of flash drought in the eastern United States. *Agricultural and Forest Meteorology*, 247, 414–423. <https://doi.org/10.1016/j.agrformet.2017.08.031>.
- Ford, T.W., Mcroberts, D.B., Quiring, S.M. and Hall, R.E. (2015) On the utility of in situ soil moisture observations for flash drought early warning in Oklahoma, USA. *Geophysical Research Letters*, 42, 9790–9798. <https://doi.org/10.1002/2015GL066600>.
- Forthofer, R. N., and Lehnen, R. G. (1981). *Rank Correlation Methods*. In: *Public Program Analysis*. Boston, MA: Springer US.
- González-Hidalgo, J., Vicente-Serrano, S., Peña-Angulo, D., Salinas, C., Tomas-Burguera, M. and Beguería, S. (2018) High-resolution spatio-temporal analyses of drought episodes in the western Mediterranean basin (Spanish mainland, Iberian Peninsula). *Acta Geophysica*, 66, 381–392. <https://doi.org/10.1007/s11600-018-0138-x>.
- Hao, Z. and Aghakouchak, A. (2013) Multivariate standardized drought index: a parametric multi-index model. *Advances in Water Resources*, 57, 12–18. <https://doi.org/10.1016/j.advwatres.2013.03.009>.
- Hao, Z. and Aghakouchak, A. (2014) A nonparametric multivariate multi-index drought monitoring framework. *Journal of Hydrometeorology*, 15, 89–101. <https://doi.org/10.1175/JHM-D-12-0160.1>.
- Hao, Z., Hao, F., Singh, V.P., Ouyang, W. and Cheng, H. (2017) An integrated package for drought monitoring, prediction and analysis to aid drought modeling and assessment. *Environmental Modelling and Software*, 91, 199–209. <https://doi.org/10.1016/j.envsoft.2017.02.008>.
- Hao, Z., Hao, F., Singh, V.P., Xia, Y., Ouyang, W. and Shen, X. (2016) A theoretical drought classification method for the multivariate drought index based on distribution properties of standardized drought indices. *Advances in Water Resources*, 92, 240–247. <https://doi.org/10.1016/j.advwatres.2016.04.010>.
- He, J., Yang, K., Tang, W., Lu, H., Qin, J., Chen, Y. and Li, X. (2020) The first high-resolution meteorological forcing dataset for land process studies over China. *Scientific Data*, 7, 25. <https://doi.org/10.1038/s41597-020-0369-y>.
- Koster, R.D., Schubert, S.D., Wang, H., Mahanama, S.P. and DeAngelis, A.M. (2019) Flash drought as captured by reanalysis data: disentangling the contributions of precipitation deficit and excess evapotranspiration. *Journal of Hydrometeorology*, 20, 1241–1258. <https://doi.org/10.1175/jhm-d-18-0242.1>.
- Li, B., Beaudoin, H., Rodell, M. and NASA/GSFC/HSL. 2018. GLDAS Catchment Land Surface Model L4 Daily 0.25 x 0.25 Degree V2.0. Goddard Earth Sciences Data and Information Services Center (GES DISC), Greenbelt, Maryland, USA. <https://doi.org/10.5067/LYHA9088MFWQ>.
- Li, L., She, D., Zheng, H., Lin, P. and Yang, Z.-L. (2020a) Elucidating diverse drought characteristics from two meteorological drought indices (SPI and SPEI) in China. *Journal of Hydrometeorology*, 21 (7), 1513–1530. <https://doi.org/10.1175/jhm-d-19-0290.1>.
- Li, R., Chen, N., Zhang, X., Zeng, L., Wang, X., Tang, S., Li, D. and Niyogi, D. (2020) Quantitative analysis of agricultural drought propagation process in the Yangtze River basin by using cross wavelet analysis and spatial autocorrelation. *Agricultural and Forest Meteorology*, 280, 107809–101530. <https://doi.org/10.1175/jhm-d-19-0290.1>.
- Liang, H., Xue, Y., Zongshan, L., Wang, S. and Wu, X. (2018) Soil moisture decline following the plantation of *Robinia pseudo-acacia* forests: evidence from the loess plateau. *Forest Ecology and Management*, 412, 62–69. <https://doi.org/10.1016/j.foreco.2018.01.041>.
- Liu, Y., Zhu, Y., Ren, L., Otkin, J., Hunt, E.D., Yang, X., Yuan, F. and Jiang, S. (2020a) Two different methods for flash drought identification: comparison of their strengths and limitations. *Journal of Hydrometeorology*, 21, 691–704. <https://doi.org/10.1175/JHM-D-19-0088.1>.
- Liu, Y., Zhu, Y., Zhang, L., Ren, L., Yuan, F., Yang, X. and Jiang, S. (2020) Flash droughts characterization over China: from a perspective of the rapid intensification rate. *Science of the Total Environment*, 704, 135373. <https://doi.org/10.1016/j.scitotenv.2019.135373>.
- Liu, Z., Wang, Y., Shao, M., Jia, X. and Li, X. (2016) Spatiotemporal analysis of multiscale drought characteristics across the loess plateau of China. *Journal of Hydrology*, 534, 281–299.

- Mann, H.B. (1945) Nonparametric tests against trend. *Econometrica: Journal of the Econometric Society*, 13(3), 245–259. <https://doi.org/10.2307/1907187>.
- Mishra, A.K. and Desai, V.R. (2005) Drought forecasting using stochastic models. *Stochastic Environmental Research and Risk Assessment*, 19, 326–339. <https://doi.org/10.1007/s00477-005-0238-4>.
- Mishra, A.K. and Singh, V.P. (2010) A review of drought concepts. *Journal of Hydrology*, 391, 202–216. <https://doi.org/10.1016/j.jhydrol.2010.07.012>.
- Mo, K.C. and Lettenmaier, D.P. (2015) Heat wave flash droughts in decline. *Geophysical Research Letters*, 42, 2823–2829. <https://doi.org/10.1002/2015GL064018>.
- Mo, K.C. and Lettenmaier, D.P. (2016) Precipitation deficit flash droughts over the United States. *Journal of Hydrometeorology*, 17, 1169–1184. <https://doi.org/10.1175/JHM-D-15-0158.1>.
- Nam, W., Hong, E., Choi, J., Kim, T., Hayes, M. and Svoboda, M. (2017) Assessment of the extreme 2014~2015 drought events in North Korea using weekly standardized precipitation evapotranspiration index (SPEI). *Journal of The Korean Society of Agricultural Engineers*, 59, 65–74.
- Otkin, J.A., Anderson, M.C., Hain, C. and Svoboda, M. (2013) Examining the relationship between drought development and rapid changes in the evaporative stress index. *Journal of Hydrometeorology*, 15, 938–956. <https://doi.org/10.1175/JHM-D-13-0110.1>.
- Otkin, J.A., Anderson, M.C., Hain, C.R., Mladenova, I.E., Basara, J. B. and Svoboda, M. (2013) Examining rapid onset drought development using the thermal infrared-based evaporative stress index. *Journal of Hydrometeorology*, 14, 1057–1074. <https://doi.org/10.1175/JHM-D-12-0144.1>.
- Otkin, J.A., Anderson, M.C., Hain, C.R., Svoboda, M., Johnson, D. K., Mueller, R., Tadesse, T., Wardlow, B.D. and Brown, J.F. (2016) Assessing the evolution of soil moisture and vegetation conditions during the 2012 United States flash drought. *Agricultural and Forest Meteorology*, 218, 230–242. <https://doi.org/10.1016/j.agrformet.2015.12.065>.
- Otkin, J.A., Mark, S., Hunt, E.H., Trent, W.F., Martha, C.A., Christopher, R.H. and Basara, J.B. (2018) Flash droughts: a review and assessment of the challenges imposed by rapid-onset droughts in the United States. *Bulletin of the American Meteorological Society*, 99, 911–919. <https://doi.org/10.1016/j.agrformet.2015.12.065>.
- Pendergrass, A.G., Meehl, G.A., Pulwarty, R., Hobbins, M., Hoell, A., AghaKouchak, A., Bonfils, C.J.W., Gallant, A.J.E., Hoerling, M., Hoffmann, D., Kaatz, L., Lehner, F., Llewellyn, D., Mote, P., Neale, R.B., Overpeck, J.T., Sheffield, A., Stahl, K., Svoboda, M., Wheeler, M.C., Wood, A. W. and Woodhouse, C.A. (2020) Flash droughts present a new challenge for subseasonal-to-seasonal prediction. *Nature Climate Change*, 10, 191–199. <https://doi.org/10.1038/s41558-020-0709-0>.
- Rajsekhar, D., Singh, V.P. and Mishra, A.K. (2015) Multivariate drought index: an information theory based approach for integrated drought assessment. *Journal of Hydrology*, 526, 164–182. <https://doi.org/10.1016/j.jhydrol.2014.11.031>.
- Ren, Y., Shi, Y., Wang, J., Li, Y., Zhu, Y., Yang, Z. and Wei, B. (2013) Spatial and temporal variation characteristics of drought in northwestern China during 1961–2009 with standardized precipitation index (in Chinese). *Journal of Glaciology and Geocryology*, 35, 938–948. <https://doi.org/10.7522/j.issn.1000-0240.2013.0106>.
- Rodell, M., Houser, P.R., Jambor, U., Gottschalck, J., Mitchell, K., Meng, C., Arsenault, K., Cosgrove, B., Radakovich, J., Bosilovich, M., Entin, J.K., Walker, J.P., Lohmann, D. and Toll, D. (2004) The global land data assimilation system. *Bulletin of the American Meteorological Society*, 85, 381–394. <https://doi.org/10.1175/BAMS-85-3-381>.
- She, D. and Xia, J. (2013) The spatial and temporal analysis of dry spells in the Yellow River basin, China. *Stochastic Environmental Research and Risk Assessment*, 27, 29–42. <https://doi.org/10.1007/s00477-011-0553-x>.
- She, D. and Xia, J. (2018) Copulas-based drought characteristics analysis and risk assessment across the loess plateau of China. *Water Resources Management*, 32, 547–564. <https://doi.org/10.1007/s11269-017-1826-z>.
- Sheffield, J., Goteti, G. and Wood, E.F. (2006) Development of a 50-year high-resolution global dataset of meteorological forcings for land surface modeling. *Journal of Climate*, 19, 3088–3111. <https://doi.org/10.1029/2002JD003274>.
- Svoboda, M., Lecomte, D., Hayes, M.J., Heim, R.R., Gleason, K.L., Angel, J.R., Rippey, B., Tinker, R., Palecki, M. and Stooksbury, D.E. (2002) The drought monitor. *Bulletin of the American Meteorological Society*, 83, 1181–1190. <https://doi.org/10.1175/1520-0477-83.8.1181>.
- Vicente-Serrano, S.M., Begueria, S. and Lopezmoreno, J.I. (2010) A multiscalar drought index sensitive to global warming: the standardized precipitation evapotranspiration index. *Journal of Climate*, 23, 1696–1718. <https://doi.org/10.1175/2009JCLI2909.1>.
- Vicente-Serrano, S.M., Tomasburguera, M., Begueria, S., Reig, F., Latorre, B., Penagallardo, M., Luna, M.Y., Morata, A. and Gonzalezhidalgo, J.C., 2017. A high resolution dataset of drought indices for Spain, international conference on data technologies and applications, 22. https://doi.org/10.3390/data2030022_2.
- Wang, G., Huang, J., Guo, W., Zuo, J., Wang, J., Bi, J., Huang, Z. and Shi, J. (2010) Observation analysis of land-atmosphere interactions over the loess plateau of Northwest China. *Journal of Geophysical Research: Atmospheres*, 115(D00K17). <https://doi.org/10.1029/2009JD013372>.
- Wang, G., Zhang, P., Liang, L. and Zhang, S. (2017) Evaluation of precipitation from CMORPH, GPCP-2, TRMM 3B43, GPCC, and ITPCAS with ground-based measurements in the Qinling-Daba Mountains, China. *PLoS One*, 12, e0185147. <https://doi.org/10.1371/journal.pone.0185147>.
- Wang, L. and Yuan, X. (2018) Two types of flash drought and their connections with seasonal drought. *Advances in Atmospheric Sciences*, 35, 1478–1490. <https://doi.org/10.1007/s00376-018-8047-0>.
- Wang, L., Yuan, X., Xie, Z., Wu, P. and Li, Y. (2016) Increasing flash droughts over China during the recent global warming hiatus. *Scientific Reports*, 6, 30571. <https://doi.org/10.1038/srep30571>.
- Wang, L.N., Zhu, Q.K., Zhao, W.J. and Zhao, X.K. (2015) The drought trend and its relationship with rainfall intensity in the loess plateau of China. *Natural Hazards*, 77, 479–495. <https://doi.org/10.1007/s11069-015-1594-0>.
- Wang, S., Fu, B., Chen, H. and Liu, Y. (2018) Regional development boundary of China's loess plateau: water limit and land

- shortage. *Land Use Policy*, 74, 130–136. <https://doi.org/10.1016/j.landusepol.2017.03.003>.
- Wang, W., Cui, W., Wang, X. and Chen, X. (2016) Evaluation of GLDAS-1 and GLDAS-2 forcing data and Noah model simulations over China at the monthly scale. *Journal of Hydrometeorology*, 17, 2815–2833. <https://doi.org/10.1175/JHM-D-15-0191.1>.
- Wilks, D.S. (2011) *Statistical Methods in the Atmospheric Sciences*. San Diego, CA: Academic Press.
- Wu, J., Miao, C., Zheng, H., Duan, Q., Lei, X. and Li, H. (2018) Meteorological and hydrological drought on the loess plateau, China: evolutionary characteristics, impact, and propagation. *Journal of Geophysical Research: Atmospheres*, 123, 569–584. <https://doi.org/10.1029/2018JD029145>.
- Xia, Y., Hao, Z., Shi, C., Li, Y., Meng, J., Xu, T., Wu, X. and Zhang, B. (2019) Regional and global land data assimilation systems: innovations, challenges, and prospects. *Journal of Meteorological Research*, 33, 159–189. <https://doi.org/10.1007/s13351-019-8172-4>.
- Yang, F., Lu, H., Yang, K., He, J., Wang, W., Wright, J.S., Li, C., Han, M. and Li, Y. (2017) Evaluation of multiple forcing data sets for precipitation and shortwave radiation over major land areas of China. *Hydrology and Earth System Sciences*, 21, 5805–5821. <https://doi.org/10.5194/hess-21-5805-2017>.
- Yang, K. and He, J. 2018. China meteorological forcing dataset (1979-2018) in: Cente, N.T.P.D. (Ed.).
- Yang, K., He, J., Tang, W.J., Qin, J. and Cheng, C.C.K. (2010) On downward shortwave and longwave radiations over high altitude regions: observation and modeling in the Tibetan plateau. *Agricultural and Forest Meteorology*, 150, 38–46. <https://doi.org/10.1016/j.agrformet.2009.08.004>.
- Yuan, X., Wang, L., Wu, P., Ji, P., Sheffield, J. and Zhang, M. (2019) Anthropogenic shift towards higher risk of flash drought over China. *Nature Communications*, 10, 4661. <https://doi.org/10.1038/s41467-019-12692-7>.
- Zhang, B., Wu, P., Zhao, X., Wang, Y., Wang, J. and Shi, Y. (2012) Drought variation trends in different subregions of the Chinese loess plateau over the past four decades. *Agricultural Water Management*, 115, 167–177. <https://doi.org/10.1016/j.agwat.2012.09.004>.
- Zhang, S., Yang, D., Yang, Y., Piao, S., Yang, H., Lei, H. and Fu, B. (2018) Excessive afforestation and soil drying on China's loess plateau. *Journal of Geophysical Research: Biogeosciences*, 123, 923–935. <https://doi.org/10.1002/2017JG004038>.
- Zhang, Y., You, Q., Chen, C. and Li, X. (2017) Flash droughts in a typical humid and subtropical basin: a case study in the Gan River basin, China. *Journal of Hydrology*, 551, 162–176. <https://doi.org/10.1016/j.jhydrol.2017.05.044>.
- Zhao, A., Zhang, A., Liu, J., Feng, L. and Zhao, Y. (2019) Assessing the effects of drought and “grain for green” program on vegetation dynamics in China's loess plateau from 2000 to 2014. *Catena*, 175, 446–455. <https://doi.org/10.1016/j.catena.2019.01.013>.
- Zhu, Z. and Shi, C. (2014) Simulation and evaluation of CLDAS and GLDAS soil moisture data in China (in Chinese). *Science Technology and Engineering*, 14, 1671–1815.

SUPPORTING INFORMATION

Additional supporting information may be found online in the Supporting Information section at the end of this article.

How to cite this article: Hu, C., Xia, J., She, D., Li, L., Song, Z., & Hong, S. (2021). A new framework for the identification of flash drought: Multivariable and probabilistic statistic perspectives. *International Journal of Climatology*, 1–17. <https://doi.org/10.1002/joc.7157>